**International Journal of Environmental Sciences**
ISSN: 2229-7359
Vol. 11 No.23s, 2025
https://www.theaspd.com/ijes.php

# Quinoxaline from Marine Mangrove (*Rhizophora apiculata*) Exhibits Anti-Metastatic Potential against B16F-10 Melanoma Cells in In-Vitro and In-Vivo Models

**Meshak Dhanashekaran Cecileya Jasmin[1,2], Venugopal Vinod Prabhu[2], Perumal Elangovan[3] Kunnathur Murugesan Sakthivel[4] and Narayanaswamy Radhakrishnan[1]*.**
[1]*Department of Biochemistry, Saveetha Medical College and Hospital, Saveetha Institute of Medical and Technical Sciences (Deemed to be University), Thandalam, Chennai, Tamil Nadu 602105, India.
[2]Department of Microbiology, School of Sciences, P P Savani University, Dhamdod, Kosamba, Surat, Gujarat 394125, India.
[3]Agilus Diagnostic Laboratory (SRL Limited formerly), Ashok Nagar, Chennai, Tamil Nadu 600083, India.
[4]Department of Biochemistry, PSG College of Arts & Science, Coimbatore, Tamil Nadu 614014, India.

***Abstract:***
***Background:*** *Lung cancer remains the leading cause of cancer related mortality worldwide, with non-small cell lung carcinoma (NSCLC) representing the most prevalent and aggressive subtype due to its high metastatic potential. Despite therapeutic advances, current treatment options are often insufficient, underscoring the need for novel anti-metastatic strategies.*
***Objective:*** *This study investigates the anti-metastatic potential of a quinoxaline in a B16F-10melanoma-induced experimental lung metastasis model in BALB/c mice.*
***Methods:*** *Mice were administered quinoxaline (10 mg/kg body weight, intraperitoneally), and its effects on lung metastasis, survival, biochemical markers and matrix metalloproteinases (MMPs) were assessed. Molecular docking studies were also performed to evaluate the compound's interaction with MMP-2 and MMP-9.*
***Results:*** *Quinoxaline treatment resulted in a significant reduction ($p < 0.01$) in the number of lung metastatic nodules and enhanced survival rates in treated mice. The compound effectively restored the levels of metastatic biomarkers, including hydroxyproline, uronic acid, hexosamine, gamma-glutamyl transpeptidase (GGT), nitric oxide (NO) and sialic acid, towards normal physiological ranges. Molecular docking studies further revealed strong inhibitory interactions of quinoxaline with MMP-2 and MMP-9, supporting its role in suppressing extracellular matrix degradation and tumor cell invasion.*
***Conclusion:*** *Our findings demonstrate that quinoxaline exhibits potent anti-metastatic activity by modulating metastatic biomarkers and inhibiting MMP activity, suggesting its potential as a promising therapeutic agent for the management of lung cancer metastasis.*
***Keywords:*** *Quinoxaline, lung metastasis, matrix metalloproteinases, anti-metastatic therapy, lung cancer, metastatic biomarkers*

## 1. INTRODUCTION:

Cancer is the second foremost source of fatality worldwide contributing to approximately 9.6 million fatalities in 2018, which equates to 1 in every 6 deaths. Lung cancer is the most frequently diagnosed cancer in men, followed by prostate and colorectal cancers. Among women, the most commonly occurring cancers are breast, colorectal, lung, cervical, and thyroid cancers. Lung cancer remains one of the leading causes of cancer incidence and mortality worldwide, posing a significant public health concern. Statistics indicate a rise in cancer-related deaths since 2012, with 1.6 million fatalities and 1.8 million new cases reported [1]. Lung cancer remains the most commonly diagnosed cancer and is the leading cause of cancer-related mortality among both men and women [2].Lung cancer represents a significant challenge to public health because of its high prevalence and mortality rates. Based on histopathological findings, lung cancer is broadly classified into (NSCLC) and small cell lung carcinoma (SCLC). NSCLC is the majority making up approximately 85% of all lung cancer incidences [3].
Metastasis, the migration of cancer cells to organs far from the primary origin site, represents the severe stage of cancer. Most cancer associated deaths occur due to complications arising from metastatic disease rather than the primary tumor itself [3,4]. Metastasis can be categorized into three interconnected phases—dissemination, dormancy, and colonization each of which may overlap in time. These phases represent a series of events collectively known as the metastatic stream, where these cells occupy tissues, survive during transit and establish colonies in distant organs. During dissemination, tumor cells with oncogenic driver mutations breach the

basement membrane, penetrating deeper tissue layers and adapting to survive without niche-specific growth factors. Subsequently, these cells enter nearby blood vessels or lymphatic systems (intravasation) and later exit into distant organs (extravasation) through mechanisms like transendothelial migration, capillary disruption, neuronal migration, or local spread into adjacent compartments such as the pleural or peritoneal cavities [4]. Metastases were the primary cause of treatment breakdown among lung cancer patients. It involves movement of malignant tumor to distant locations through various pathways from lungs. The most frequent metastatic sites for lung cancer include brain, bones, lymph nodes and liver [5].The exact mechanisms underlying lung cancer metastasis remain insufficiently understood. Generally, the metastatic process in lung cancer cells followed detachment of cells from the extracellular matrix (ECM) followed by near site migration with invasion and extravasation at the metastatic place and proliferation to establish secondary tumor [6].

The process of lung cancer metastasis is highly intricate, involving dynamic interactions within the tumor microenvironment and the functional role of lung cancer stem cells (LCSCs) [7].Critical mechanisms such as epithelial mesenchymal transition (EMT), along with angiogenesis and lymphangiogenesis, are pivotal in driving the progression of metastatic disease [8]. The microenvironment comprises cancer cells, stromal cells and the (ECM), which together support tumor growth and development. According to Xie et al [9] stromal components, including fibroblasts, immune cells and vascular endothelial cells, actively contribute to the metastatic potential of lung cancer. Currently, lung cancer treatment relies on surgery, radiation, chemotherapy, and targeted therapy. Despite these diverse approaches, the clinical outcomes remain suboptimal. Over the past several decades, in general survival time for lung cancer has shown little improvement, and it remains to be the foremost reason of cancer associated deaths. As a result, there is growing interest among clinicians and researchers in exploring the potential of compounds as effective anti-lung cancer agents [10].

Quinoxaline ($C_8H_6N_2$), also known as 1,4-diazanaphthalene or benzopyrazine which are highly effective nitrogenous heterocyclic materials comprising with benzene ring merged with a pyrazine ring shown in Figure 1. Quinoxaline derivatives exert diverse range of biological activities, including antibacterial, antifungal, anticancer, antiviral and anti-protozoal properties. Moreover, these derivatives serve as crucial intermediates in organic synthesis. Several commercially available drugs incorporate the quinoxaline scaffold, such as echinomycin (with nucleic acid inhibitory properties), triostins (cyclic depsipeptides with anti-bacterial activity), dioxidine and mequindox (anti-bacterial agents)and panadipion (hepato-protective agent). Furthermore, quinoxaline-based compounds exhibit other therapeutic effects, including anti-cardiac, anti-tuberculosis, and anti-schistosomal activities [11-14].Numerous quinoxaline analogues with diverse biological functions, along with their synthetic methodologies, have been patented globally, highlighting their significance in medicinal chemistry [13].

Quinoxaline has been identified as a prominent compound in the extract of *Rhizophora apiculata* (Mangrove) through LC-MS analysis, which confirmed its abundance and highlighted its anti-cancer potential [15-17]. While quinoxaline is known to contain numerous polyphenolic compounds associated with various health benefits, its anti-metastatic activity remains unreported. Therefore this study focused on examining and confirming the anti-metastatic properties of quinoxaline, offering novel insights into its therapeutic potential. This research evaluated the anti-metastatic efficacy of the compound in a BALB/c mouse model of lung metastasis by B16F-10 melanoma cells.

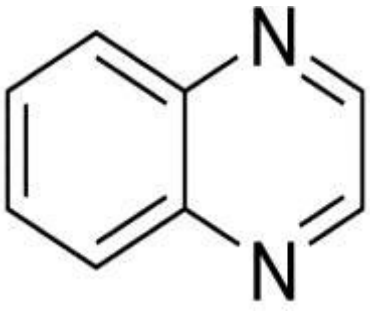


**Figure 1:**($C_8H_6N_2$) quinoxaline**,** an aromatic heterocyclic compound composed of a fused benzene and pyrazine ring.

## 2. MATERIAL AND METHODS

### 2.1 Chemical and Reagents

Dulbecco's Modified Eagle's Medium, Antibiotics (streptomycin and penicillin-G), L-glutamine, PBS (Phosphate-Buffered Saline), trypsin-EDTA, Acridine Orange, Ethidium Bromide, Sodium Dodecyl Sulfate (SDS), trypan blue, Ethylene diamine tetra acetic Acid (EDTA), Rhodamine-123, Triton X-100, ethanol, dimethyl sulfoxide (DMSO) and bovine serum albumin. Quinoxaline, with a purity of 98%, was sourced from Sigma Aldrich Chemicals Pvt. Ltd. (USA). All other chemicals used wereof analytical gradeprocured from Hi-Media Laboratories Pvt. Ltd. (India).

### 2.2 Experimental animals

Male BALB/c mice, 4–6 weeks old and weighing 22–25 g, were housed in a sterile, air-controlled environment. The facility was maintained at a stable temperature of 24°C with approximately 50% relative moisture and a 12-hour light/dark cycle. The animals were provided with unrestricted access to mouse chow, drinking water, proper bedding, nesting materials and daily monitoring for sign of distress throughout the experiment. All experimental procedures adhered to the guidelines and policies established by the Institutional Animal Ethics Committee (IAEC), Committee for Control and Supervision of Experiments on Animals (CCSEA), Government of India, Project Approval No: JJC/BC/AH/014/2024.

### 2.3 Cell Culture

B16F10 murine melanoma cell line was procured from National Centre for Cell Sciences, Pune, India. DMEM were used for this cell line maintenance along with 10% fetal bovine serum (FBS). Antibiotics - Penicillin (100 U/ml), and Streptomycin of (100 µg/ml) in order to avoid bacterial contaminations. The cell lines were maintained with 5% $CO_2$ at 37°C.

### 2.4 MTT assay

The MTT assay was conducted to evaluate the cytotoxicity of quinoxaline on B16F10 cells using the method described by Mosmann (1983) [18]. Cells were seeded in 96-well plates at a density of 5,000–10,000 cells per well and incubated for 24 hours. Later, the cells were treated with quinoxaline at concentrations ranging from 1 µg/ml to 500 µg/ml and incubated for 24, 48, or 72 hours. Following treatment, MTT solution was added to each well and incubated for 3–4 hours. The resulting formazan crystals were dissolved in DMSO, and absorbance was measured at 570 nm. Cell viability was calculated, and the IC50 value was determined. For *in vivo* experiments, the selected concentration of quinoxaline was re-suspended in 1% (w/v) vehicle (gum acacia) and administered through intraperitoneal (i.p.) injection at a dose of 10 mg/kg body weight (b.wt) for 10 consecutive days. [19-22].

### 2.5 Biochemical analysis

The BALB/c mice were separated as two groups with 9 animals each, to conduct the study. Metastasis was induced in all mice by administration of $1\times10^6$ B16F10 melanoma cells through the lateral tail vein injection. Group I served as the untreated control group received vehicle only. Group II was treated with quinoxaline at a dosage of 10 mg/kg body weight (b.w.) through (i.p.) injection for 10 consecutive days. At various time intervals (7th, 11th, and 21st days), mice were euthanized and blood sample were collected. The serum was separated and analyzed for biochemical markers include Sialic acid levels, Nitric oxide (NO), and Gamma-Glutamyl Transferase (GGT) activity.

### 2.6 Evaluation of the impact of quinoxaline on serum sialic acid levels in mice with metastatic tumors

To assess the impact of quinoxaline on serum sialic acid levels in metastatic tumor-bearing mice, the animals were separated into two groups (9 mice per group). Metastasis was induced in mice by administration of $1 \times 10^6$ B16F10 melanoma cells into the lateral tail vein as per standard procedure. Group I served as the metastasis induced untreated control (received only vehicle), Group II was administered with quinoxaline (i.p.) for 10 consecutive days. On day 21, blood was collected via cardiac puncture and serum was separated for analysis. Sialic acid levels were measured using the Thiobarbituric acid (TBA) assay [23-24]. Serum samples were hydrolyzed with 0.2 N sulfuric acid, followed by oxidation with periodic acid and incubated at 37°C for a minute. The oxidation process was halted with sodium arsenate, and a 6% thiobarbituric acid solution was added. Sialic acid levels were determined spectrophotometrically at 549 nm, using a reference at 532 nm, after addition of Dimethyl Sulfoxide (DMSO). The concentration of sialic acid was calculated using a standard curve prepared with N-acetylneuraminic acid.

### 2.7 Evaluation of the impact of quinoxaline on serum GGT levels and NO activity in metastatic tumor-bearing mice

GGT levels were measured on different time pointsthe 7th, 11th, and 21st days. The assay quantified the release of p-nitroaniline from gamma-glutamyl-p-nitroaniline in the presence of glycylglycine. GGT activity was determined by comparing the results to a standard curve generated using p-nitroaniline as reference [25]. To evaluate the activity of quinoxaline on serum nitric oxide (NO) levels in metastatic tumor bearing animals, serum NO was measured on the 7, 11 and 21$^{st}$days using the Griess reagent-based method. A reaction mixture containing sodium nitroprusside and serum was incubated at 25°C for 2 hour 30 minutes. After incubation, 1 ml of the mixture was combined with an equal volume of Griess reagent and incubated at room temperature for around 20 minutes. The absorbance of the resulting pink-colored chromophore was measured at 546 nm. NO levels were then quantified and expressed in micromoles [26].

### 2.8 Evaluation of the impact of quinoxaline on lung Collagen Hydroxyproline, Hexosamine, Uronic acid level and tumor nodule count

BALB/c mice were divided into two groups, each consisting of 9 animals. Metastasis was induced in all mice by injecting metastatic B16F10 melanoma cells ($1 \times 10^6$ cells per animal) via injection through lateral tail vein. Group I served as the metastasis induced untreated control animals received only vehicle and Group II was administered with quinoxaline (i.p.) for ten consecutive days. On the final day of the experiment (Day 21), all animals were euthanized. Lung tissues were excised for tumor nodule counting and subsequent biochemical analysis. The lung samples were evaluated for hydroxylproline content [27], hexosamine levels and uronic acid content [28-29]. This study to examine the effect of quinoxaline on biochemical markers related to lung health and tumor progression.

### 2.9 Evaluate the effect of quinoxaline on lung collagen hydroxyproline levels in metastatic tumor-bearing mice

Lung collagen hydroxyproline was measured as per standard method described by [27]. Lung tissues of100 mg were homogenized followed by proteins precipitation with trichloroacetic acid (TCA). The precipitate was hydrolyzed in sealed glass tubes with 6 N HCl for 24 hours at 110°C. Following hydrolysis, the hydrochloric acid was evaporated and the residual hydrolysate was thoroughly dried. The remains were dissolved in water and were analyzed using the chloramine-T method. Optimal density was precise at 560 nm, and the hydroxyproline content was determined with the absorbance with a standard curve prepared using reagent-grade hydroxyproline. This assay provided a quantitative measure of lung collagen levels, reflecting the effect of quinoxaline treatment on collagen deposition in metastatic tumor bearing animals.

### 2.10 Evaluation of the impact of quinoxaline on lung hexosamine level in metastatic tumor-bearing BALB/c mice

Hexosamine levels in lung tissue were measured using the method described by [28]. Lung tissue specimen were lyophilized and then hydrolyzed in sealed glass tubes with 2 N HCl at 100°C for 6 hours. After hydrolysis, the residue was thoroughly dried, and the remaining material was dissolved in water and then treated with 2% acetyl acetone. The hexosamine content was measured by adding Ehrlich's reagent, and the absorbance was captured at 530 nm. A standard curve was prepared using glucosamine as the standard. This procedure provided an accurate quantification of lung hexosamine levels, offering insights into the biochemical impact of quinoxaline treatment of metastatic tumor bearing animals.

### 2.11 Evaluation of the impact of quinoxaline on lung uronic acid level in metastatic tumor-bearing BALB/c mice

The uronic acid content in lung tissues was determined using the carbazole reaction method [29]. Approximately 100 mg of lung tissue was homogenized and digested with crude papain (125 µg/mL) in 0.1 M sodium acetate buffer (pH 6.0) containing 5 mM EDTA and 5 mM cysteine hydrochloride. Digestion was carried out at 60°C for 18 hours. Following digestion, 0.5 mL of the sample was mixed with 3 mL of concentrated sulfuric acid (analytical grade, slowly added under cooling conditions), then the mixture was hydrolyzed by heating at 100°C for 20 minutes in sealed glass tubes. After cooling to room temperature, 0.1 mL of freshly prepared 0.125% carbazole solution (in absolute ethanol) was added to each tube, and the samples were incubated at room temperature for 30 minutes in the dark. Absorbance was read at 530 nm using a spectrophotometer. A standard

curve was generated using glucuronic acid lactone (Sigma-Aldrich) at concentrations ranging from 5 to 50 µg/mL, treated under identical conditions. Uronic acid levels were expressed as µg/mg tissue, reflecting ECM remodeling activity in the lung tissues.

### 2.12 Evaluation of the impact of quinoxaline on the survival rate of metastatic tumor-bearing BALB/c mice

The impact of quinoxaline on the survival rate of animals bearing metastatic tumors was evaluated by monitoring the remaining animals (n=3) in each experimental group. The death of each animal was tracked, and the increase in life span (% ILS) was determined by formula: % ILS = (T - C) / C × 100. In this formula, T denotes the survival duration of the treated animals, and C represents the survival duration of the control group. This approach facilitated the assessment of quinoxaline's effectiveness in prolonging the survival of animals with metastatic tumors.

### 2.13 Evaluation of quinoxaline on inhibition of lung metastatic nodule formation

Lung metastatic nodules were visualized and counted using the Indian ink injection method. The excised lungs are gently washed with phosphate-buffered saline (PBS), followed by tracheal injection of Indian ink to stain normal lung tissue, leaving metastatic nodules as pale, ink-excluded spots; fixed lungs were cleared using benzyl alcohol-benzyl benzoate (BABB) and nodules were counted under a stereomicroscope, as described by Sato and Yamada (1984) [65].

### 2.14 Histopathological analysis of tumor metastatic lung tissue

Lung tissue samples collected from the animals were fixed in 10% formalin, then sliced into 5-µm thick sections and stained with hematoxylin and eosin (H&E).The stained slides were analyzed under a microscope to identify histopathological changes, including large metastatic lesions, hyperchromatic nuclei and pleomorphism.

### 2.15 Evaluation of Interactions between the ligand (quinoxaline) and the two target proteins (a-MMP-2, b-MMP-9) Using the SwissDock Method

**Preparation of Ligands**

The chemical structure of the ligand quinoxaline (CID No: 7045) was obtained from the PubChem database. The ligand was prepared using ChemDraw software for both two-dimensional and three-dimensional structural representations. The three-dimensional (3D) structure of quinoxaline was then subjected to further analysis using SwissDock (SD) for molecular docking studies.

### 2.16 Identification and preparation of target enzymes

The three-dimensional structures of Matrix Metalloproteinase 2 (1QIB) and Matrix Metalloproteinase 9 (4H1Q) were obtained from the Protein Data Bank. The "A" chain of each protein was isolated by eliminating the other chains, ligands (heteroatoms), and crystallographic water molecules using UCSF Chimera software (Regents, University of California, San Francisco, USA [30].

### 2.17 Molecular Docking

Molecular docking analysis of quinoxaline (ligand) was carried out using the SwissDock web server. SwissDock is a widely used online tool for predicting the binding affinities and docking poses of ligands with target macromolecules, such as MMP-2 and MMP-9. The best docked pose was determined by conducting a binding site study, which was visualized using PyMOL [31].

### 2.18 Statistical analysis

The data are expressed as mean ± standard deviation (SD). Statistical analysis was performed using one-way analysis of variance (ANOVA), followed by Dunnett's test for multiple comparisons. All statistical computations were conducted with GraphPad Instat software (Version 3.0; GraphPad Software, San Diego, CA). A*p-value* of less than 0.05 was considered as statistically significant.

## 3. RESULTS

### 3.1 Cytotoxic effect of quinoxaline on B16F10 melanoma cells

Cells were treated with increasing concentrations of quinoxaline, ranging from 1 µg/ml to 500 µg/ml and incubated for 24, 48, and 72 hours. A dose-dependent decrease in cell viability was observed. The half-maximal

inhibitory concentration (IC50) was determined and used to identify effective dose. Consequently, a non-toxic dose of 10 mg/kg body weight was chosen for animal studies and administered via intraperitoneal injection over 10 days (Figure 2).

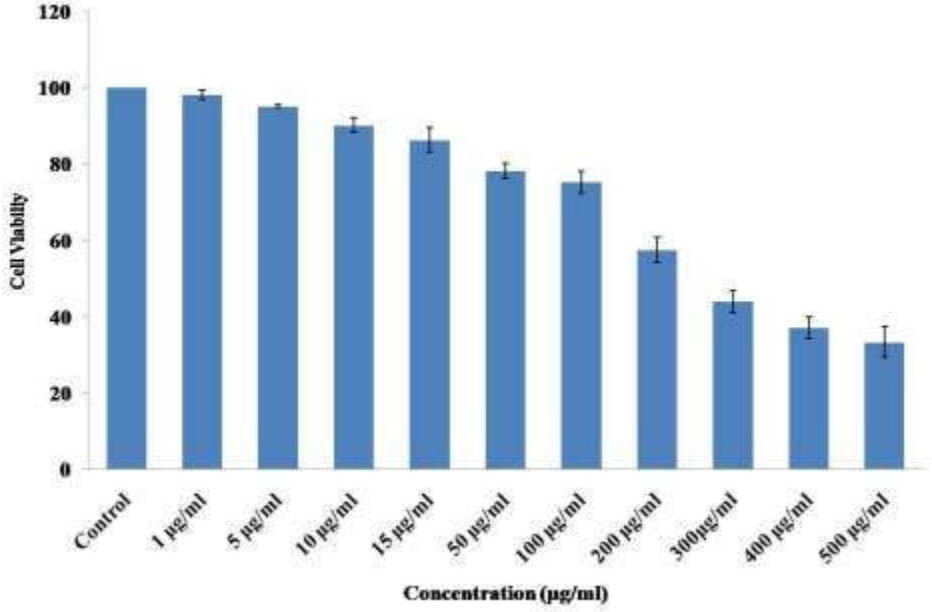


**Figure 2:** MTT assay, the cytotoxicity of quinoxaline tested on B16F-10 cells which were determined by the cell viability assay and the half maximal inhibitory concentration ($IC_{50}$) values were calculated and the optimum doses were analyzed at different time period.

### 3.2 Effect of quinoxaline on the serum GGT and NO level of metastatic tumor bearing animals

The effects of quinoxaline on lung and serum GGT and NO levels in metastatic tumor-bearing animals are summarized in Figure 3 and 4. Quinoxaline administration resulted in a significant ($p< 0.01$) reduction in serum GGT levels to 52.20 ± 2.1 nmol p-nitroaniline/ml on the 21st day, compared to 93.24 ± 6.1 nmol p-nitroaniline/ml in the metastasis control group on the same day. Additionally, quinoxaline treatment drastically ($p< 0.01$) decrease serum NO levels to 25.30 ± 0.21 µM on the 21st day, compared to 36.30 ± 0.25 µM in the metastasis control group.

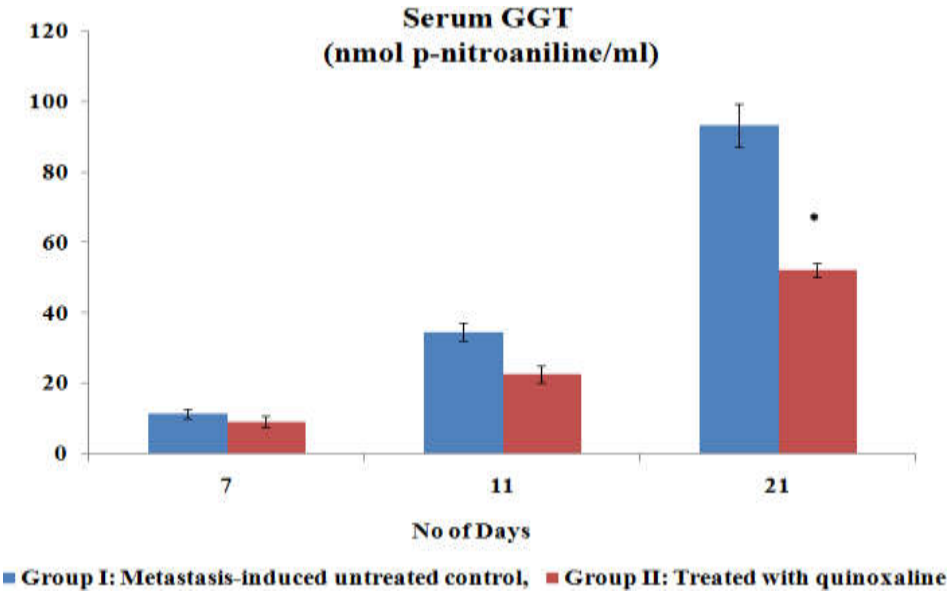


**Figure 3:** The effect of quinoxaline on lung and serum GGT level in metastases tumor bearing animals is shown here. Treatment BALB/c animals received quinoxaline (10mg/kg b.wt.(ip)) for 10 consecutive days and metastatic control received metastatic B16F-10 melanoma cells ($1x10^6$cells/animal) via lateral tail vein and received only vehicle. Blood samples were collected by tail vein on 7th,11th and (cardiac puncture) 21st day.

Serum samples were isolated to determine GGT. Value is significantly different from metastasis untreated control (*$p$<0.05) (n=6). Values are expressed as mean ± SD.

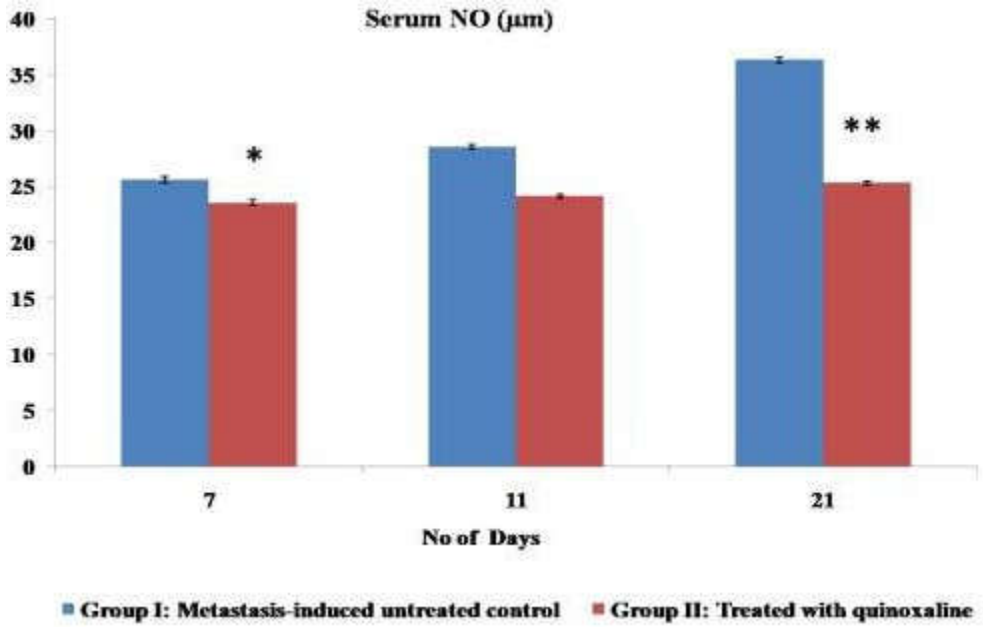


**Figure 4:** The effect of quinoxaline on lung and serum NO level in metastases tumor bearing animals is shown here. Treatment BALB/c animals received quinoxaline (10mg/kg b.wt. (ip) for 10 consecutive days and metastatic control received metastatic B16F-10 melanoma cells ($1x10^6$cells/animal) via lateral tail vein and received only vehicle. Blood samples were collected by tail vein on 7th, 11th and (cardiac puncture) 21st day. Serum samples were isolated to determine NO. Value is significantly different from metastasis untreated control (*$p$<0.05), (**$p$<0.01) (n=6). Values are expressed as mean ± SD.

**3.3 Effect of quinoxaline on serum sialic acid, lung hydroxyproline, hexoamine and uronic acid of metastases bearing animals**

The activity of quinoxaline on serum sialic acid, lung hydroxyproline, hexosamine, and uronic acid levels in metastatic tumor-bearing animals is summarized in Figure 5. The administration of quinoxaline resulted in a significant ($p$< 0.01) reduction in serum sialic acid levels (28.21 ± 0.23 µg/ml) compared to the metastasis control group (95.20 ± 0.52 µg/ml). Similarly, quinoxaline treatment significantly ($p$< 0.01) decreased lung hydroxyproline levels (8.23 ± 0.12 µg/mg protein) in comparison to the metastatic control group (25.13 ± 0.15 µg/mg protein).

In quinoxaline-treated animals, lung hexosamine levels were extensively reduced ($p$ < 0.01) to 3.13 ± 0.12 mg per 100 mg of dry tissue weight compare to the metastatic control group, which recorded 10.01 ± 0.11 mg per 100 mg of dry tissue weight. Similarly, a significant reduction ($p$ < 0.01) in lung uronic acid levels was observed in quinoxaline-treated animals, with levels measured at 86.10 ± 3.12 µg per 100 mg, wet tissue weight, compared to 223.10 ± 3.13 µg per 100 mg, wet tissue weight in the metastatic control group. These findings emphasize the ability of quinoxaline to counteract the biochemical changes associated with metastasis.

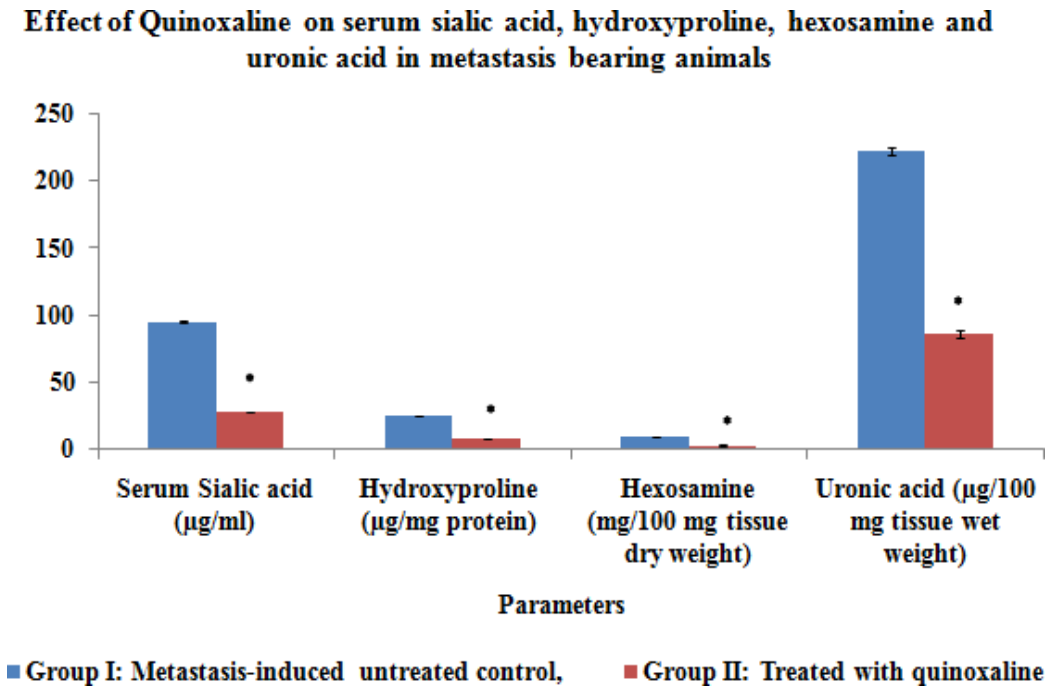


**Figure 5:** The effect of quinoxaline on serum sialic acid, lung hydroxyproline, hexoamine and uronic acid in metastases bearing animals is shown here. Treatment BALB/c animals received quinoxaline (10mg/kg b.wt. (ip) for 10 consecutive days and metastatic induced untreated control received B16F-10 melanoma cells ($1x10^6$cells/animal) via lateral tail vein. Blood samples were collected 21st day by cardiac puncture and serum samples were isolated to determine silaic acid level. On the same day lungs were dissected to determine the lung hydroxyproline, hexoamine and uronic acid level. Value is significantly different from metastasis untreated control (*$p$<0.05) (n=6). Values are expressed as mean ± SD.

### 3.4 Effect of quinoxaline on inhibition of lung metastatic nodule formation and on survival of animals

The impact of quinoxaline on lung metastatic nodule formation and animal survival is summarized in Table 1. The study utilized B16F-10 melanoma cells known for inducing lung tumors in experimental models [32]. Quinoxaline action resulted in a significant ($p < 0.01$) decrease in the number of visible pulmonary tumor nodules, with treated mice showing 20.2 ± 1.4 nodules compared to 38.1 ± 1.2 nodules in the metastasis control group. This corresponds to a 53% reduction in lung nodule formation. Furthermore, quinoxaline administration significantly enhanced the continued life rate of treated animals, extending their maximum survival period to 70 ± 1.5 days, whereas metastasis control animals survived for only 33 ± 1.2 days. The percentage increase life span (% ILS) was determined using the formula % ILS = (T − C) / C × 100, where T represents the survival days of the treated group and C those of the control group. The % ILS for quinoxaline-treated animals was calculated to be 112.1%, reflecting a notable improvement in both survival time and overall life span.

| Treatment | No of tumor nodules | No of days survived |
|---|---|---|
| **Group I: Metastasis-induced untreated control** | 38.1 ± 1.2 | 33 ± 1.2 |
| **Group II: Treated with quinoxaline** | 20.2± 1.4** | 70 ± 1.5** |

**Table 1:** Effect of quinoxaline on inhibition of lung metastatic nodule formation and on survival of animals Treatment BALB/c animals received quinoxaline (10mg/kg b.wt. (ip) for 10 consecutive days and metastatic untreated control received B16F-10 melanoma cells ($1x10^6$cells/animal) via lateral tail vein and received only vehicle. On 21st day the animals were euthanized and lungs were dissected and lung metastatic nodules were counted. The percentage increase in life span is calculated by (T-C/Cx100), where T and C are the number of days survived by the treated animals and metastatic control animals respectively. Value is significantly different from metastasis untreated control (**$p$<0.01). Values are expressed as mean ± SD.

### 3.5 Histopathological analysis

The histopathological analysis of lung tissue from animals with metastatic tumors is shown in Figure 6. Representative images were taken from lung specimen collected at the conclusion of the experimental period (Day 21). The (Figure 6A) represent the normal lung cell architecture and (Figure 6B) represent the metastatic untreated control group were prominent metastases were evident and characterized by extensive tumor nodules, hyperchromatic nuclei, and areas of necrosis. In contrast, lung tissue from metastatic tumor-bearing animals treated with quinoxaline (Figure 6C) showed notably smaller metastases, emphasizing the ability of quinoxaline to inhibit metastatic progression.

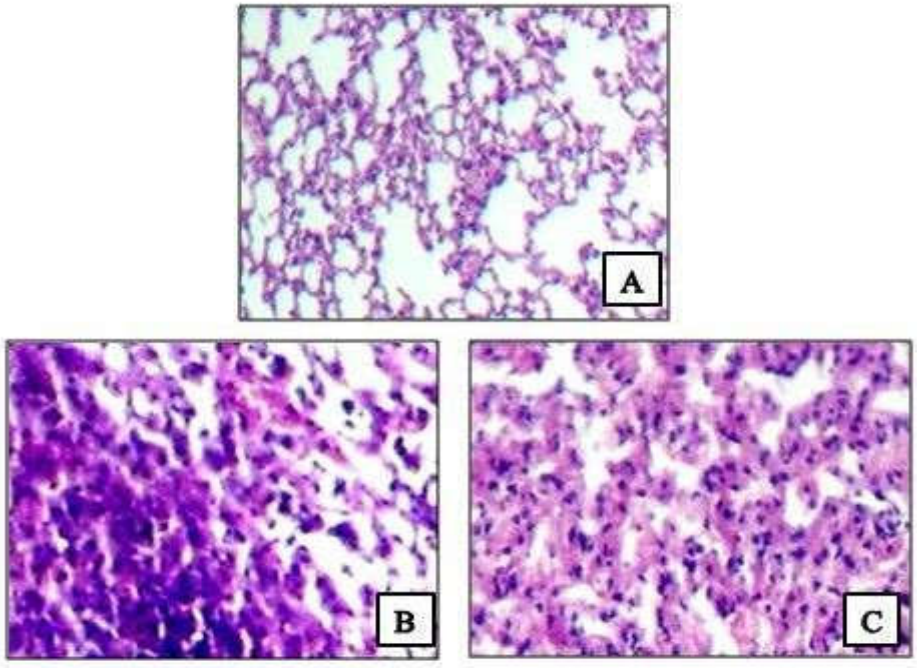


**Figure 6:** Histopathology of lung metastatic of tumor bearing BALB/c animals. A portion of excised lung tissue from lung metastatic tumor induced BALB/c animals were fixed in 10% formalin, cut into 5-µm thickness, stained using H&E (hematoxylin and eosin) and then examined for histopathological changes. **(A)** Normal lung cell architecture. **(B)** Metastatic induced untreated control BALB/c animals shows40x large metastasis surrounding a vessel. The cells show hyperchromatic nucleus and pleomorphism. **(C)** Metastatic induced treated with quinoxaline,40x lungs showing small metastasis. The cells show hyperchromatic nucleus and pleomorphism.

**3.6 Molecular Docking**

The docking analysis of quinoxaline with MMP-2 and MMP-9 revealed strong interactions at their respective binding sites. The best-docked pose for each enzyme showed stable binding, with key residues in both enzymes forming significant interactions with the ligand. The results indicate that quinoxaline has a potential affinity for these target enzymes, suggesting its possible role as an inhibitor or modulator in relevant biochemical pathways. The interaction patterns, including hydrogen bonds and hydrophobic interactions, were clearly visualized using PyMOL, providing insight into the molecular basis of ligand bindingis shown in Table 2 and Figure 7.

| Ligand name | Swissdock binding energy (-kcal/mol) | Interactions of amino acids residues | Bond distance (A°) |
|---|---|---|---|
| **Matrix metalloproteinase-2 (MMP-2)** | | | |
| Quinoxaline | 6.16 | Ala220 | 3.2 |
| **Matrix metalloproteinase-9 (MMP-9)** | | | |
| Quinoxaline | 6.39 | Tyr245 | 3.2 |

**Table 2:** Docking study of quinoxaline with MMP-2 and MMP-9: Molecular docking analysis of quinoxaline (ligand) was carried out using the SwissDock web server.

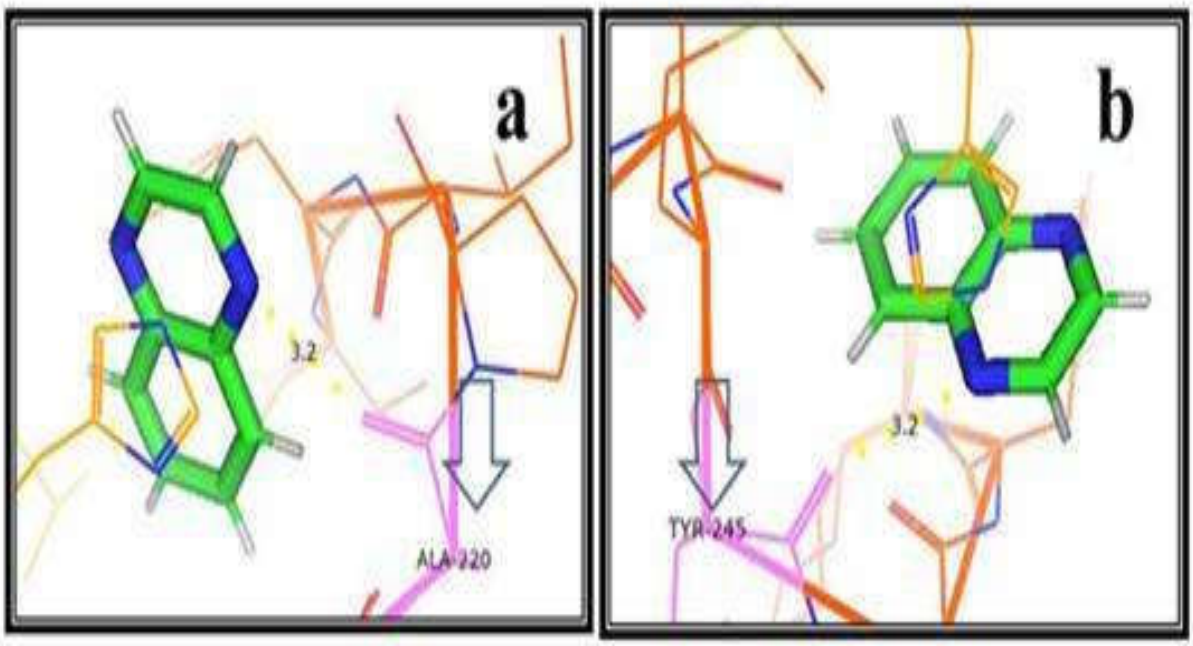


**Figure 7:** Demonstrating the Interaction of the ligand (Quinoxaline) with Target Enzymes (a-MMP-2 and b-MMP-9) Using the SwissDock Method

## 4 DISCUSSION:

Cancer typically arises in epithelial tissues, where disruptions in cell-cell and cell-matrix interactions occur during tumor progression. During this process, neoplastic cells transition into mesenchymal-like cells, characterized by a loss of cell-cell adhesion, altered morphology, and the ability to migrate to distant organs [33]. Metastasis denotes to the complex process through which cancer cells spread from a primary tumor to distant sites. This process involves several cellular mechanisms, including invasion of the surrounding stroma, evasion of immune surveillance by suppressing anti-tumorigenic responses, and the development of resistance to therapeutic interventions [34-36]. While some cells in the primary tumor may exhibit proliferative activity, those undergoing EMT often reduce proliferation as they disseminate [37].Disseminated cells that survive in distant organs can eventually lead to micro metastases [38]. Colonization of far tissues by these disseminated tumor cells is highly ineffective. Although circulating tumor cells (CTCs) can be detected in the blood of cancer patients at concentrations exceeding 1000 CTCs/ml of plasma, only a small proportion of these cells contribute to detectable metastases [39-41]. Among the various metastatic cancers, the lung is the primary organ encounter by tumor cells, making it a common place for metastatic spread [42]. It has been reported that the endurancetime for patients with metastatic melanoma are below 10% [43]. Treatment options for tumor metastasis include surgery, radiotherapy, chemotherapy, and hormone therapies [44].The choice of management for metastasis depends on factors such as the type of primary cancer the size and the site of the metastatic lesions. Given the complexity of metastasis and the limited effectiveness of current treatments, which are often associated with low survival rates [43], metastasis remains a critical target in cancer therapy. The present study exhibited the anti-metastatic effect of quinoxaline against the B16F-10 metastatic lung cancer cells both *in vitro* and *in vivo* as well. NO is a signaling molecule intricate in the both physiological and pathological processes [45]. Over the past two decades, its role in cancer progression and metastasis has been extensively studied [46]. NO promotes cancer growth and metastasis [47] and is produced from L-arginine and oxygen by nitric oxide synthases (NOS), with varying NOS expression in tumors affecting metastasis [48]. NO is implicated in nearly all stages of cancer metastasis [49]. For example, in melanoma cells, NO enhances the expression of matrix metalloproteinases (MMPs) through the MAPK (ERK/p38) pathway, aiding tumor spread [50].NO also facilitates metastasis by inhibiting integrin-mediated platelet adhesion, stimulating α9β1 integrin, and inducing iNOS expression, which promotes cell migration and invasion [51]. In hepatocellular carcinoma, iNOS modulates MMP-9 expression, supporting angiogenesis and metastasis [52].Furthermore, higher NOS activity is linked to increased angiogenesis in head and neck cancer [53] while NO aids in tumor intravasation and activates hypoxia-inducible factor-1 (HIF-1), which promote tumor progression via the PI3k/Akt pathway [54-55,66].

In this study, quinoxaline significantly reduced nitric oxide (NO) production, thereby inhibiting the metastatic potential of tumor cells in experimental mice. This protective effect was further demonstrated by around 50% reduction in lung tumor nodules compared to the metastatic control group. The decrease in tumor nodules was also associated by a 112% raise in the survival rate of the metastatic bearing animals. GGT, the enzyme responsible for cleaving the γ-glutamyl-cysteine peptide bond in glutathione (GSH) and other γ-glutamyl compounds, plays a key role in providing energy to tumor cells via the gamma-glutamyl cycle. Increased GGT levels are commonly observed in human tumors and are associated with tumor cell proliferation. In a study involving 322 patients, 65 out of 82 patients showed GGT positivity in serum and tumors, with higher tumor GGT expression linked to lymph node metastasis. Kaplan-Meier analysis revealed that patients with high tumor GGT levels had significantly shorter overall survival [56].Elevated serum GGT levels are also predictive of poor survival and cancer recurrence. Serum GGT levels increase during tumor progression because of cellular proliferation, which makes it a dependable marker for cell growth [57]. In this study, the administration of quinoxaline led to a significant decrease in serum GGT level in metastatic tumor-bearing animals, suggesting a suppression of tumor cell proliferation and metastasis.

Sialic acid, a derivative of neuraminic acid, is a terminal component of carbohydrate chains on glycoproteins. It plays a crucial role in cellular adhesion, acting as a component of various cell surface receptors and serving as a site for cellular recognition, particularly during the invasion of foreign cells, including cancer cells. Metastatic cancer cells often exhibit an increased expression of sialic acid-rich glycoproteins [58-59].Under normal conditions, serum sialic acid levels remain constant, but when cells undergo malignant transformation, sialic acid is shed from the cell surface and enters the bloodstream. This process, known as hypersialylation, leads to an increase in sialic acid metabolism, which promotes tumor progression. In this study, quinoxaline treatment significantly reduced serum sialic acid levels in metastatic tumor-bearing animals. By inhibiting the expression of sialic acid on the surface of malignant cells, quinoxaline prevents electrostatic repulsion and reduces metastasis. The reduction in serum sialic acid levels was directly correlated with a decrease in metastasis. Additionally, hydroxyproline (a non-essential amino acid) which is found in collagen and other extracellular proteins. It plays a key role in collagen synthesis and in thermodynamic stability of the triple-helical structure of collagen and its related tissues [60]. Lung hydroxyproline levels are commonly used as a standard indicator to assess collagen content and lung fibrosis [61]. The administration of quinoxaline in the present study led to a significant reduction in lung hydroxyproline levels in metastatic tumor-bearing animals, thereby preventing excessive collagen deposition and inhibiting the pulmonary fibrosis typically associated with lung metastasis.

The hexosamine biosynthetic pathway (HBP) is a key metabolic pathway involved in sensing the cellular metabolic state. It relies on various molecules, including glucose, glutamine, UTP, and acetate, and is regulated by enzymes that have a critical role in cancer pathophysiology. Previous literatures suggests that the activation of the HBPcould serve as a cancer biomarker and Inhibition of HBP enzymes can enhance the sensitivity of tumor cells to conventional therapies [62]. Changes in HBP flux, influenced by nutrient availability or cytokines, can impact protein O-GlcNAcylation and glycosylation. Although the full scope of HBP's influence on tumor behavior is not completely understood, some studies have explored the relationship between this pathway and cancer cell biology, particularly through its rate-limiting enzyme [63].

In this study, quinoxaline treatment led to a considerable decrease in lung hexosamine levels in metastatic tumor bearing animals. By inhibiting the excessive synthesis of hexosamine and blocking the extracellular matrix (ECM), quinoxaline effectively prevented metastasis [57].The elevated hexosamine levels in control metastatic tumor-bearing animals indicate active tumor cell growth and proliferation [64]. Quinoxaline administration resulted in a marked decrease in hydroxyproline, uronic acid, and hexosamine level in tumor-bearing mice, which correlates with reduced lung fibrosis. This finding aligns with histopathological analysis, which reported to be reduction in tumor nodules in quinoxaline-treated mice.

Matrix metalloproteinases (MMPs), especially MMP-2 and MMP-9, are crucial in cancer metastasis due to their role in degrading extracellular matrix (ECM) components. These enzymes facilitate the invasion of cancer cells by breaking down ECM barriers, allowing tumor cells to enter the bloodstream or lymphatic system and spread to distant organs. MMP-2 and MMP-9 primarily degrade type IV and type V collagen, major components of the basement membrane, thereby promoting tumor microenvironment disintegration and enhancing cancer cell migration.

In lung cancer, increased MMP-2 and MMP-9 expression correlates with poor prognosis, as their activity accelerates tumor spread and secondary lesion formation. Elevated MMP levels are often seen in advanced, metastatic stages of the disease. Our docking analysis suggests that quinoxaline may inhibit MMP-2 and MMP-9

by binding to their active sites. This inhibition could reduce ECM degradation, preventing cancer cell invasion and metastasis, and potentially improving patient outcomes in lung cancer.

In conclusion, the current study demonstrated that administration of quinoxaline, when given concurrently with tumor inoculation, significantly reduced lung colonization. Treatment with quinoxaline also resulted in a notable increase in the lifespan of BALB/c mice bearing metastatic lung tumors. These findings were consistent with the observed changes in key markers, such as lung hydroxyproline, a major component of collagen, as well as structural monosaccharides like uronic acid and hexosamine, which promote metastasis. Additionally, quinoxaline treatment reversed serum levels of GGT, a marker of cellular proliferation, as well as levels of NO and sialic acid, bringing them closer to normal. The role of quinoxaline in our docking analysis suggests a potential therapeutic approach for preventing metastasis. This study represents the first information on the anti-metastatic potential of quinoxaline in metastatic tumor bearing BALB/c animal model. Therefore, quinoxaline may serve as a promising therapeutic agent for inhibiting metastasis during tumor progression. Further research is needed to fully elucidate the mechanism underlying its anti-metastatic effects.

**ACKNOWLEDGEMENT:** Authors would like to thank management for their support to provide infrastructure to carry out this study.

**CONFLICT OF INTEREST**: The author(s) do not have any conflict of interest.

**REFERENCES**

1. Bray F, Ferlay J, Soerjomataram I, Siegel RL, Torre LA, Jemal A. Global cancer statistics 2018: GLOBOCAN estimates of incidence and mortality worldwide for 36 cancers in 185 countries. CA Cancer J Clin. 2018; 68(6):394-424.
2. Nasim F, Sabath BF, Eapen GA. Lung Cancer. Med Clin North Am. 2019;103(3):463-473.
3. Mittal V. Epithelial Mesenchymal Transition in Aggressive Lung Cancers. Adv Exp Med Biol. 2016;890:37-56.
4. McArdle JR, Siegel MD. Clinics in Chest Medicine. Preface. Clin Chest Med. 2009 Mar;30(1):xiii.
5. Tamura T, Kurishima K, Nakazawa K, Kagohashi K, Ishikawa H, Satoh H, Hizawa N. Specific organ metastases and survival in metastatic non-small-cell lung cancer. Mol Clin Oncol. 2015 Jan;3(1):217-221.
6. Chanvorachote P, Chamni S, Ninsontia C, Phiboonchaiyanan PP. Potential Anti-metastasis Natural Compounds for Lung Cancer. Anticancer Res. 2016;36(11):5707-5717.
7. Heng WS, Gosens R, Kruyt FAE. Lung cancer stem cells: origin, features, maintenance mechanisms and therapeutic targeting. BiochemPharmacol. 2019;160:121-133.
8. Yang M, Arai E, Takahashi Y, Totsuka H, Chiku S, Taniguchi H, Katai H, Sakamoto H, Yoshida T, Kanai Y. Cooperative participation of epigenomic and genomic alterations in the clinicopathological diversity of gastric adenocarcinomas: significance of cell adhesion and epithelial-mesenchymal transition-related signaling pathways. Carcinogenesis. 2020;13;41(11):1473-1484.
9. Xie S, Wu Z, Qi Y, Wu B, Zhu X. The metastasizing mechanisms of lung cancer: Recent advances and therapeutic challenges. Biomed Pharmacother. 2021;138:111450.
10. V VP, C G. Protective effect of marine mangrove Rhizophora apiculata on acetic acid induced experimental colitis by regulating anti-oxidant enzymes, inflammatory mediators and nuclear factor-kappa B subunits. Int Immunopharmacol. 2014;18(1):124-34.
11. Pan Y, Li P, Xie S, Tao Y, Chen D, Dai M, Hao H, Huang L, Wang Y, Wang L, Liu Z, Yuan Z. Synthesis, 3D-QSAR analysis and biological evaluation of quinoxaline 1,4-di-N-oxide derivatives as antituberculosis agents. Bioorg Med Chem Lett. 2016; 15;26(16):4146-53.
12. Padalino G, El-Sakkary N, Liu LJ, Liu C, Harte DSG, Barnes RE, Sayers E, Forde-Thomas J, Whiteland H, Bassetto M, Ferla S, Johnson G, Jones AT, Caffrey CR, Chalmers I, Brancale A, Hoffmann KF. Anti-schistosomal activities of quinoxaline-containing compounds: From hit identification to lead optimisation. Eur J Med Chem. 2021;15;226:113823.
13. Sharma A, Deep A, Marwaha MG, Marwaha RK. Quinoxaline: A Chemical Moiety with Spectrum of Interesting Biological Activities. Mini Rev Med Chem. 2022;22(6):927-948.
14. Palos I, González-González A, Paz-González AD, Espinoza-Hicks JC, Bandyopadhyay D, Paniagua-Castro N, Galeana-Salazar MS, Castañeda-Sánchez JI, Luna-Herrera J, Rivera G. Quinoxaline 1,4-di-*N*-oxide Derivatives as New Antinocardial Agents. Molecules. 2024; 30;29(19):4652.
15. Vinod Prabhu V, C G. Protective effect of marine mangrove Rhizophora apiculata on acetic acid induced experimental colitis by regulating anti-oxidant enzymes, inflammatory mediators and nuclear factor-kappa B subunits.IntImmunopharmacol. 2014;18(1):124-34.
16. VinodPrabhu V, Elangovan P, Niranjali Devaraj S, Sakthivel KM. Targeting apoptosis by 1,2-diazole through regulation of EGFR, Bcl-2 and CDK-2 mediated signaling pathway in human non-small cell lung carcinoma A549 cells.Gene. 2018; 30;679:352-359.
17. VinodPrabhu V, Elangovan P, Niranjali Devaraj S, Sakthivel KM. Targeting NF-κB mediated cell signaling pathway and inflammatory mediators by 1,2-diazole in A549 cells *in vitro*.Biotechnol Rep (Amst). 2021; 28;29:e00594.
18. Mosmann T. Rapid colorimetric assay for cellular growth and survival: application to proliferation and cytotoxicity assays. J Immunol Methods. 1983; 16;65(1-2):55-63.
19. Mokkhasmit M, Ngarmwathana W, Sawasdimongkol K, Permphiphat U. Pharmacological evaluation of Thai medicinal plants. J Med Assoc Thai. 1971;;54(7):490-503.
20. Cole FH Jr, Miller MP, Jones CV. Transdiaphragmatic intercostal hernia. Ann Thorac Surg. 1986;41(5):565-6.

21. Kuttan R, Bhanumathy P, Nirmala K, George MC. Potential anticancer activity of turmeric (Curcuma longa). Cancer Lett. 1985;29(2):197-202.
22. .Prabhu VV, Guruvayoorappan C. Anti-inflammatory and anti-tumor activity of the marine mangrove Rhizophora apiculata. J Immunotoxicol. 2012;9(4):341-52.
23. Skoza L, Mohos S. Stable thiobarbituric acid chromophore with dimethyl sulphoxide. Application to sialic acid assay in analytical de-O-acetylation. Biochem J. 1976; 1;159(3):457-62.
24. Bhavanandan VP. Glycosaminoglycans of cultured human fetal uveal melanocytes and comparison with those produced by cultured human melanoma cells. Biochemistry. 1981; 15;20(19):5595-602.
25. Tate SS, Meister A (1974). Inhibition of gamma glutamyl transpeptidase amino acids, peptides and derivatives and analogs of glutathione. *J Biochem*, 23, 1602.
26. Green LC, Wagner DA, Glogowski J, et al (1982). Analysis of nitrate, nitrite and (15N) nitrate in biological fluids. *Anal Biochem*, 126, 131-8.
27. Bergman I, Loxley R (1970). The determination of hydroxyproline in urine hydrosylates. *Clin. Chem Acta*, 27, 347-9.
28. Elson LA, Morgan WT. A colorimetric method for the determination of glucosamine and chondrosamine. Biochem J. 1933;27(6):1824-8.
29. Bitter T, Muir HM (1962). A modified uronic acid carbazole reaction. Anal. *Biochem*, 4, 330-34.
30. Kumaraswamy S, Arumugam G, Pandurangan AK, Prabhakaran VS, Narayanaswamy R. Molecular docking analysis of organic acids (OA) from honey as modulators of human ferritin, transferrin, and hepcidin. J MicrobiolBiotechnol Food Sci. 2023: 12(5):e5743).
31. Grosdidier A, Zoete V, Michielin O. SwissDock, a protein-small molecule docking web service based on EADock DSS. Nucleic Acids Res. 2011;;39(Web Server issue):W270-7.
32. Engbrin JA, Hoffman MP, Karmand AJ, Kleinman HK (2002). The B16F-10 receptor for a metastasis promoting site on Laminin-1 is a heparan sulfate/ chondroitin sulfate containing proteoglycan. Cancer Res, 62, 3549-54.
33. Bacac M, Stamenkovic I. Metastatic cancer cell. Annu Rev Pathol. 2008;3:221–47.
34. Fischer KR, Durrans A, Lee S, Sheng J, Li F, Wong ST, Choi H, El Rayes T, Ryu S, Troeger J, et al. (2015). Epithelial-to-mesenchymal transition is not required for lung metastasis but contributes to chemoresistance. Nature 527, 472–476.
35. Kalluri R (2016). The biology and function of fibroblasts in cancer. Nat Rev Cancer 16, 582–598.
36. Massagué J, Obenauf AC. Metastatic colonization by circulating tumour cells. Nature. 2016; 21;529(7586):298-306.
37. Rojas-Puentes L, Cardona AF, Carranza H, Vargas C, Jaramillo LF, Zea D, Cetina L, Wills B, Ruiz-Garcia E, and Arrieta O (2016). Epithelial-mesenchymal transition, proliferation, and angiogenesis in locally advanced cervical cancer treated with chemoradiotherapy. Cancer Med 5, 1989–1999.
38. Harper KL, Sosa MS, Entenberg D, Hosseini H, Cheung JF, Nobre R, Avivar-Valderas A, Nagi C, Girnius N, Davis RJ, Farias EF, Condeelis J, Klein CA, Aguirre-Ghiso JA. Mechanism of early dissemination and metastasis in Her2$^{+}$ mammary cancer. Nature. 2016 ; 22;540(7634):588-592.
39. Nagrath S, Sequist LV, Maheswaran S, Bell DW, Irimia D, Ulkus L, Smith MR, Kwak EL, Digumarthy S, Muzikansky A, et al. (2007). Isolation of rare circulating tumour cells in cancer patients by microchip technology. Nature 450, 1235–1239.
40. Suhail Y, Cain MP, Vanaja K, Kurywchak PA, Levchenko A, Kalluri R, Kshitiz. Systems Biology of Cancer Metastasis. Cell Syst. 2019 Aug 28;9(2):109-127.
41. van Maaren MC, de Munck L, de Bock GH, Jobsen JJ, van Dalen T, Linn SC, Poortmans P, Strobbe LJA, Siesling S. 10 year survival after breast-conserving surgery plus radiotherapy compared with mastectomy in early breast cancer in the Netherlands: a population-based study. Lancet Oncol. 2016;17(8):1158-1170.
42. Hyoudou K, Nishikawa M, Kobayashi Y, Umeyama Y, Yamashita F, Hashida M. PEGylated catalase prevents metastatic tumor growth aggravated by tumor removal. Free Radic Biol Med. 2006; 1;41(9):1449-58.
43. Bhatia J, Parish A. Nutrition and the lung. Neonatology. 2009;95(4):362-7.
44. Wang Q, Shu X, Dong Y, Zhou J, Teng R, Shen J, Chen Y, Dong M, Zhang W, Huang Y, Xie S, Wei Q, Zhao W, Chen W, Yuan X, Qi X, Wang L. Tumor and serum gamma-glutamyl transpeptidase, new prognostic and molecular interpretation of an old biomarker in gastric cancer. Oncotarget. 2017; 30;8(22):36171-36184.
45. Coulter JA, McCarthy HO, Xiang J, Roedl W, Wagner E, Robson T, Hirst DG. Nitric oxide--a novel therapeutic for cancer. Nitric Oxide. 2008;19(2):192-8.
46. Wink DA, Vodovotz Y, Laval J, Laval F, Dewhirst MW, Mitchell JB. The multifaceted roles of nitric oxide in cancer. Carcinogenesis. 1998;19(5):711–721.
47. Bing RJ, Miyataka M, Rich KA, Hanson N, Wang X, Slosser HD, Shi SR. Nitric oxide, prostanoids, cyclooxygenase, and angiogenesis in colon and breast cancer. Clin Cancer Res. 2001;7(11):3385–3392.
48. Radomski MW, Jenkins DC, Holmes L, Moncada S. Human colorectal adenocarcinoma cells: differential nitric oxide synthesis determines their ability to aggregate platelets. Cancer Res. 1991;51(22):6073–6078.
49. Fidler IJ. The pathogenesis of cancer metastasis: the 'seed and soil' hypothesis revisited. Nat Rev Cancer. 2003;3(6):453–458.
50. Ishii Y, Ogura T, Tatemichi M, Fujisawa H, Otsuka F, Esumi H. Induction of matrix metalloproteinase gene transcription by nitric oxide and mechanisms of MMP-1 gene induction in human melanoma cell lines. Int J Cancer. 2003;103(2):161–168.
51. Gupta SK, Vlahakis NE. Integrin alpha9beta1 mediates enhanced cell migration through nitric oxide synthase activity regulated by Src tyrosine kinase. J Cell Sci. 2009;122(Pt 12):2043–2054.
52. Sun MH, Han XC, Jia MK, Jiang WD, Wang M, Zhang H, Han G, Jiang Y. Expressions of inducible nitric oxide synthase and matrix metalloproteinase-9 and their effects on angiogenesis and progression of hepatocellular carcinoma. World J Gastroenterol. 2005;11(38):5931–5937.
53. Jiang T, Yu JT, Zhu XC, Zhang QQ, Tan MS, Cao L, Wang HF, Lu J, Gao Q, Zhang YD, et al. Angiotensin-(1–7) Induces Cerebral Ischemic Tolerance by Promoting Brain Angiogenesis in a Mas/eNOS-Dependent Pathway. Br J Pharmacol. 2014;171,18:4222-32.
54. Bessa X, Elizalde JI, Mitjans F, Pinol V, Miquel R, Panes J, Piulats J, Pique JM, Castells A. Leukocyte recruitment in colon cancer: role of cell adhesion molecules, nitric oxide, and transforming growth factor beta1. Gastroenterology. 2002;122(4):1122–1132.

55. Cheng H, Wang L, Mollica M, Re AT, Wu S, Zuo L. Nitric oxide in cancer metastasis. Cancer Lett. 2014 ; 10;353(1):1-7.
56. Wang Q, Shu X, Dong Y, Zhou J, Teng R, Shen J, Chen Y, Dong M, Zhang W, Huang Y, Xie S, Wei Q, Zhao W, Chen W, Yuan X, Qi X, Wang L. Tumor and serum gamma-glutamyl transpeptidase, new prognostic and molecular interpretation of an old biomarker in gastric cancer. Oncotarget. 2017; 30;8(22):36171-36184.
57. Pradeep,Kuttan (2002). Effect of piperine on the inhibition of lung metastasis induced B16F-10 melanoma cells in mice. Clinical & Experimental Metastasis, 19: 703-708.
58. Fuster Mark M, Esko Jeffrey D (2005). The sweet and sour of cancer: Glycans as novel therapeutic targets. Nature Reviews Cancer,5: 526–542.
59. Berghuis AY, Pijnenborg JFA, Boltje TJ, Pijnenborg JMA. Sialic acids in gynecological cancer development and progression: impact on diagnosis and treatment. Int J Cancer. 2022;150(4):678–687.
60. Srivastava AK, Khare P, Nagar HK, Raghuwanshi N, Srivastava R. Hydroxyproline: A Potential Biochemical Marker and Its Role in the Pathogenesis of Different Diseases. Curr Protein Pept Sci. 2016;17(6):596-602.
61. Voet D, Voet JG. Biochemistry, New York: John Wiley, 1995;157-258.
62. Lam C, Low JY, Tran PT, Wang H. The hexosamine biosynthetic pathway and cancer: Current knowledge and future therapeutic strategies. Cancer Lett. 2021 Apr 10;503:11-18.
63. Carvalho-Cruz P, Alisson-Silva F, Todeschini AR, Dias WB. Cellular glycosylation senses metabolic changes and modulates cell plasticity during epithelial to mesenchymal transition. Dev Dyn. (2017) 247:481–91..
64. West DC, Hampson IN, Arnold F, et al. Angiogenesis induced by degradationproducts of hyaluronic acid. Science,1985; 228, 1324-1326.
65. Sato, S., & Yamada, Y. A new method for the visualization of metastatic nodules in the lung of mice using Indian ink injection. Japanese Journal of Cancer Research,1984;75(9), 889–895.
66. Sakthivel KM, et al. Nano encapsulated polymeric Scopoletin suppresses the progression of colorectal cancer by regulating cytokines and inflammatory mediators in AOM/DSS murine model. Biochemical and Biophysical Research Communications, 2025;769, 151973.